Published in final edited form as:
Science. 2019 February 22; 363(6429): 875–880. doi:10.1126/science.aav0569.

A Pharmacological Master Key Mechanism that Unlocks the Selectivity Filter Gate in K^+ Channels

Marcus Schewe[#1,*], **Han Sun**[#2], **Ümit Mert**[1], **Alexandra Mackenzie**[3,4,5], **Ashley C. W. Pike**[3], **Friederike Schulz**[1], **Cristina Constantin**[6,7], **Kirsty S. Vowinkel**[8], **Linus J. Conrad**[4,5], **Aytug K. Kiper**[8], **Wendy Gonzalez**[9,10], **Marianne Musinszki**[1], **Marie Tegtmeier**[1], **David C. Pryde**[11], **Hassane Belabed**[12], **Marc Nazare**[12], **Bert L. de Groot**[13], **Niels Decher**[8], **Bernd Fakler**[6,7], **Elisabeth P. Carpenter**[3,4], **Stephen J. Tucker**[4,5], **Thomas Baukrowitz**[1,*]

[1]Institute of Physiology, Christian-Albrechts University of Kiel, 24118 Kiel, Germany

[2]Leibniz-Forschungsinstitut für Molekulare Pharmakologie (FMP), Department of Structural Biology, 13125 Berlin, Germany

[3]Structural Genomics Consortium, University of Oxford, Oxford OX3 7DQ, United Kingdom

[4]OXION Initiative in Ion Channels and Disease, University of Oxford, Oxford OX1 3PN, United Kingdom

[5]Clarendon Laboratory, Department of Physics, University of Oxford, Oxford OX1 3PU, United Kingdom

[6]Institute of Physiology II, Albert-Ludwigs University of Freiburg, 79104 Freiburg, Germany

[7]Centers for Biological Signaling Studies CIBSS and BIOSS, 79104 Freiburg, Germany

[8]Institute of Physiology and Pathophysiology, Vegetative Physiology, Philipps-University of Marburg, 35037 Marburg, Germany

[9]Centro de Bioinformatica y Simulacion Molecular, Universidad de Talca, 3465548 Talca, Chile

[10]Millennium Nucleus of Ion Channels-Associated Diseases (MiNICAD), Universidad de Talca, 3465548 Talca, Chile

[*]Correspondence and requests for materials should be addressed to M.S. (m.schewe@physiologie.uni-kiel.de) or T.B. (t.baukrowitz@physiologie.uni-kiel.de).

M.S. https://orcid.org/0000-0002-6192-5651
T.B. https://orcid.org/0000-0003-4562-0505

Author contributions: M.S. and T.B. conceived the study and designed the electrophysiological experiments. M.S., Ü.M., F.S. and M.T. performed all inside-out patch-clamp experiments in *Xenopus* oocytes. M.S. and T.B. analyzed the data. M.M. designed K^+ channel mutations. C.C. performed whole-cell recordings in CHO cells and analyzed the data together with B.F. Single channel recordings in *Xenopus* oocytes were carried out and analyzed by K.V. and A.K.K. supervised by N.D. Single channel recordings in HEK293 cells were performed and analyzed by L.J.C. supervised by S.J.T. A.M. purified TREK-2 and co-crystallized TREK-2 with BL-1249^{Br}. A.M. and A.C.W.P. obtained and analysed the X-ray data supervised by E.P.C and S.J.T. D.P. synthesized the brominated BL-1249. H.B. synthesized ML67-33 supervised by M.N. H.S. designed, performed and analyzed all molecular dockings and MD simulations with critical comments of B.L.d.G. W.G. calculated and analyzed the NCA pharmacophore together with M.S. and N.D. M.S. and M.M. prepared and edited all figures. T.B. M.S., B.F., E.P.C and S.J.T. contributed to the writing and editing of the manuscript, and approved the manuscript.

Competing interests: Authors declare no competing interests.

Data and materials availability: All data is available in the main text or the supplementary materials.

Europe PMC Funders Author Manuscripts

[11]Pfizer Worldwide Medicinal Chemistry, Neuroscience and Pain Research Unit, Portway Building, Granta Park, Great Abington, Cambridgeshire CB21 6GS, United Kingdom

[12]Leibniz-Forschungsinstitut für Molekulare Pharmakologie (FMP), Department of Medicinal Chemistry, 13125 Berlin, Germany

[13]Computational Biomolecular Dynamics Group, Max Planck Institute for Biophysical Chemistry, 37077 Göttingen, Germany

[#] These authors contributed equally to this work.

Abstract

Potassium channels have been evolutionarily tuned for activation by diverse biological stimuli, and pharmacological activation is thought to target these specific gating mechanisms. Here we report a class of negatively charged activators (NCAs) that bypass the specific mechanisms but act as master keys to open K^+ channels gated at their selectivity filter (SF), including many K_{2P} channels, voltage-gated hERG channels and Ca^{2+}-activated BK-type channels. Functional analysis, X-ray crystallography and molecular dynamics simulations revealed that the NCAs bind to similar sites below the SF, increase pore and SF K^+ occupancy and open the filter gate. These results uncover an unrecognized poly-pharmacology among K^+ channel activators and highlight a filter gating machinery that is conserved across different families of K^+ channels with implications for rational drug design.

Dampening cellular electrical activity by pharmacological activation of specific types of K^+ channels has therapeutic potential for the treatment of a variety of disease states including epilepsy, arrhythmias, vascular constriction or various pain conditions (1, 2). Consequently, screening efforts have identified a number of agents that open various different types of K^+ channels (2) presumably by targeting their respective channel-specific activation mechanisms.

Distinct structural mechanisms enable K^+ channels to respond to a plethora of physiological stimuli including voltage, temperature, mechanical force, and various second messengers, such as ATP, Ca^{2+}, and H^+, as well as bioactive lipids such as PIP_2 and arachidonic acid (3, 4). However, despite this complexity, these activation pathways seem to converge on the two principal mechanisms known to gate K^+ channels open - dilation of the ‘lower’ gate at the intracellular pore entrance employed by inwardly-rectifying (K_{ir}) (5) and voltage-gated (K_v) K^+ channels (6), and activation of the selectivity filter (SF) gate used by most two-pore domain K^+ (K_{2P}) channels (4, 7, 8) and Ca^{2+}-activated (BK_{Ca}, Slo) K^+ channels (9, 10). In voltage-gated hERG channels, both mechanisms co-exist with voltage opening the lower gate, but rapid inactivation occurring through closure of the SF gate (11, 12). Here we identify a common mechanism for drug-induced channel opening that bypasses these physiological activation mechanisms in SF-gated K^+ channels.

For the mechanosensitive K_{2P} channels TREK-1 and TREK-2, the voltage-gated hERG and the Ca^{2+}-activated BK_{Ca} channels, a series of small molecule activators all harboring a negatively charged group (tetrazole or carboxylate) have been proposed to act as selective channel openers (i.e. BL-1249 for TREK-1/-2 (13); PD-118057 for hERG (14); and

NS11021 for BK_{Ca} (15)). However, application of these compounds to their respective 'non-target' channels revealed an unexpected poly-pharmacology: all three openers displayed equal efficiency in opening TREK-1 channels (Fig. 1A), hERG channels (Fig. 1B), as well as BK_{Ca} channels (Fig. 1C) whose activation curve is strongly shifted to more negative voltages (fig. S1C). This suggests they may not target channel specific activation mechanisms and may instead share a common mechanism. In all cases the compound-mediated effect was effectively antagonized by large quaternary ammonium ions (QA_L^+) such as tetra-pentyl-ammonium (TPenA) or tetra-hexyl-ammonium (THexA) that are known to block K^+ channels at a site immediately below the inner entrance to the SF (16) (Fig. 1, A and B and fig. S1C). Likewise, all these activators reduced the QA_L^+-mediated inhibition in these different K^+ channels (Fig. 1C and, figs. S1, A and B and S7, A and B). Furthermore, extended screening with BL-1249 also revealed potent activation of several other K_{2P} channels (TREK-2, TRAAK, TALK-1, TALK-2, THIK-1 and THIK-2; fig. S1D). Together, these data suggest that these negatively charged activators (termed NCAs) (BL-1249, PD-118057 and NS11021) act on a gating mechanism that is shared among these different classes of K^+ channels, and that their action involves a site that overlaps with the conserved QA_L^+-binding site located below the SF filter.

A distinctive feature of all NCA-responsive K^+ channels is their gating by the SF, a mechanism that is intimately coupled to ion permeation (17, 18). In K_{2P} channels this coupling leads to pronounced activation by Rb^+, which displays an ion occupancy distinct to K^+ at the four SF K^+ binding sites (S1 to S4) and this stabilizes the activated state of the SF gate (17). Interestingly, Rb^+ not only activated all NCA-responsive K_{2P} channels, but also led to robust activation of BK_{Ca} and hERG channels (Fig. 1D). In contrast, Rb^+ failed to exert any activatory effect on K^+ channels gated at the helix bundle-crossing (i.e. K_{ir} and most K_v channels) as was observed for $K_v1.1$, $K_v1.5$, $K_v3.1$ and $K_{ir}1.1$ (Fig. 1D); in line, these channels were also not activated by BL-1249 (fig. S2, A to E). Furthermore, CNG channels that are also gated at the SF, were not activated by BL-1249 indicating that the NCA mechanism may be specific to SF-gated K^+ channels (fig. S2F).

To gain further mechanistic insight into channel opening by the NCAs, we next investigated their binding by X-ray crystallography, cysteine-scanning mutagenesis and atomistic molecular dynamics (MD) simulations. First, anomalous diffraction data were collected from TREK-2 channels co-crystallized with a brominated derivative of BL-1249 ($BL\text{-}1249^{Br}$) (Fig. 2A and fig. S3, A to C, and supplementary materials, materials and methods). Although no discrete electron density was visible for BL-1249 itself, in anomalous difference maps two bromine peaks were clearly visible per TREK-2 dimer (fig. S3, A and B) and the mainchain protein backbone showed excellent agreement with a previously crystallized high-resolution structure of TREK-2 [Protein Data Bank (PDB) ID: 4XDJ] (19). Both bromine anomalous difference peaks were located at the entrance of the side fenestrations branching off the central pore cavity below the SF. Comparison with a structure that included QA_L^+ (16) showed these bromine positions reside within the spherical volume of THexA, but outside that of the smaller tetra-ethyl-ammonium (TEA) ion. Consistent with this, BL-1249 activation of TREK-2 channels was antagonized by THexA, but not by TEA (Fig. 2, B and C).

These structural data were complemented by cysteine-scanning mutagenesis of the pore-lining M2 and M4 helices of TREK-1. Six residues including the highly conserved P183 and L304 (also investigated in TREK-2, fig. S3D) were identified where mutations markedly reduced the apparent affinity of BL-1249. These residues cluster around the bromine densities detected in the TREK-2 co-crystal with Bl-1249^{Br} (Fig. 2D and fig. S3, C and D). A role for L304 in this presumed binding site was further supported by cysteine-modification protection experiments where the time course of irreversible pore blockade induced by application of the cysteine-modifying agent MTS-TBAO (20) to TREK-1 L304C channels was markedly slowed by the presence of BL-1249 (Fig. 2, E and F). This effect was specific for BL-1249, as two further channel activators with distinct binding sites (2-APB at the C-terminus (21) and ML335 behind the SF (22)) both failed to slow this rate (Fig. 2, E and F). Furthermore, TREK-1 activation with 2-APB or ML335 was not antagonized by QA_L^+ inhibition and mutations at the BL-1249 site did not affect 2-APB activation (figs. S4, A and B and S4E).

In addition, we performed MD simulations to examine the orientation of BL-1249^{Br} within its proposed binding site (Fig. 2G). The favoured binding pose oriented the negatively charged tetrazole group of BL-1249 towards the S6 ‘cavity binding site’ for K^+ just below the SF. The remainder of the BL-1249 molecule engaged with residues in M2 and M4 consistent with our scanning mutagenesis data (Fig. 2D and fig. S3D). Moreover, the bromine atom in these simulations was found to be within 3 - 4 Å of the bromine densities determined by crystallography (fig. S3E). Together, these data indicate binding of BL-1249 to a site below the SF and reveal a critical role of the negative charge of the acidic tetrazole ring (pKa around 5) implying a pH-dependent compound efficacy. Indeed, when tested with the K_{2P} channel TALK-2 (exhibiting little intrinsic intracellular pH (pH_i) sensitivity) BL-1249 potency dropped strongly with lowering the solution pH_i to 5 while control experiments with 2-APB lacked this pH dependence (Fig. 3F).

We have recently used atomistic MD simulations and a double-bilayer setup to study ion permeation in the TRAAK K_{2P} channel (17). We, therefore, carried out simulations of ion permeation in TRAAK with BL-1249 modelled into the equivalent site in the TRAAK channel structure [PDB ID: 4I9W] (Fig. 3A). This indicated several changes induced by BL-1249: (i) K^+ occupancy at the S6 site located adjacent to the negatively charged tetrazole group of BL-1249 increased ~16-fold (Fig. 3, A and B), (ii) increased K^+ occupancy of the S1 and S4 sites (Fig. 3B), and (iii) increased the rate of K^+ permeation by 1.6-fold (24 ± 2 ions/μs compared to 15 ± 2 ions/μs without BL-1249; Fig. 3C).

The effect of BL-1249 on ion permeation was further investigated with single channel recordings of TREK-2 expressed in HEK293 cells. Besides an increase in open probability, an increase in the measured single channel amplitude was also observed in both the inward (from -29.3 ± 1.5 pA to -34.1 ± 1.9 pA at -100 mV; n = 7) and outward (from 17.7 ± 1.3 pA to 21.7 ± 1.4 pA at +100 mV; n = 7) directions in response to BL-1249 (Fig. 3, D and E). This result is consistent with the observed increase in SF ion occupancy at S1 and S4 that is expected to enhance ion permeation via a direct knock-on effect for ions entering the SF from either side (23). A similar increase in unitary conductance was also observed for TREK-1 channels recorded in patches from *Xenopus* oocytes (fig. S4, A to C). Notably,

increases in single channel conductance have not been observed upon activation of TREK-1, TREK-2 or TRAAK K_{2P} channels by other physiological stimuli (24, 25).

Collectively, these results indicated that BL-1249 increases ion permeation and channel open probability by influencing K^+ occupancy at sites below and within the SF. In line with this notion, mutations in the SF that change filter ion occupancy at the S1 and S4 sites (17, 26) and induce the activated 'leak mode' in K_{2P} channels (17), also render them insensitive to BL-1249 (and various other activators discussed below; fig. S6, A to D).

The negatively charged moiety identified within BL-1249, PD-118057 and NS11021 is also found in a series of known activators of TREK-1/-2 K_{2P} channels (ML67-33 (27), tetrazole; DCPIB (28), carboxylate), hERG channels (PD-307243 (29), carboxylate; NS3623 (30), tetrazole) and BK_{Ca} channels (GoSlo-SR-5-6 (31), sulphonate) and its requirement for channel activation has been demonstrated for ML67-33 and GoSlo-SR-5-6 (27, 31). In fact, these compounds also share all the hallmark features of BL-1249 action, including poly-pharmacology (i.e. mutual activation of K_{2P}, BK_{Ca} and hERG channels (Fig. 4, C and D), sensitivity to QA_L^+ (Fig. 4A and fig. S7, A to C, and tables S2 and S3) and mutations that reduce BL-1249 activation in TREK-1 (fig. S4, C and D). In addition, MD simulations of their interaction with structures of the TREK-2, BK_{Ca} and hERG channel pores identified similar stable binding poses below the SF with orientation of the negative moiety towards the cavity, and a concomitant increase in K^+ occupancy at cavity and SF ion binding sites (Fig. 4, C and D, and figs. S8, A to C and S7D). Notably, this assumed NCA binding site overlaps with the 'promiscuous inhibitor binding site' in the hERG channel, which underlies drug-induced long QT syndrome (12, 32). This site is thought to accommodate many hydrophobic molecules (e.g. terfenadine) and consistent with this we found that activation by PD-118057 strongly reduced inhibition by terfenadine (Fig. 4B).

The molecular features of the NCA compounds define a common pharmacophore which, besides the negatively charged group, comprises both aromatic and hydrophobic moieties (Fig. 4E). As a control we tested tetrazole-containing compounds that do not fit this common pharmacophore on TREK-1, BK_{Ca} and hERG channels and found they were unable to promote channel activation (fig. S9, A to C).

In summary, our results uncover a class of K^+ channel openers, the NCAs, that act as a universal master-key to unlock the SF gate. Mechanistically, these NCAs bind below the SF where their negative charge promotes K^+ binding to the pore cavity and, thereby, also alter the ion occupancy in the SF in a way that is known to promote activation of the filter gate (17). We hypothesize that in particular, the increase at the S1 and S4 sites is responsible for activating the SF gate because all NCA-responsive channels are also activated by Rb^+ permeation, which is thought to increase ion occupancy at these sites, whilst mutations known to reduce S1 and S4 ion occupancy in K_{2P} channels abolish NCA activation. Furthermore, a loss of K^+ binding to the S1 site has been implicated in SF inactivation in K_v channels (33), hERG channels (32), and TREK-2 K_{2P} channels (19). However, we cannot currently exclude the possibility that non-electrostatic interactions of the NCAs with their respective binding sites also contribute to the stabilization of the active SF state as these sites involve gating sensitive regions (i.e. the TM4 (8, 19) and S6 segments (6, 34)). In any case,

our results support the view that many K_{2P} channels, as well as BK_{Ca} channels adopt a low activity (i.e. inactivated) state of their SF at rest, and that the various physiological stimuli induce structural changes that drive the SF into an active (open) state. The NCAs appear to operate via bypassing these activation mechanisms to directly stabilize the SF in its active state.

In addition, our findings have significant implications for the development of drugs that target K^+ channels as they reveal the binding sites and the mechanism of action for many established activators in various K^+ channels, and also identified the first activators for several K_{2P} channels (e.g. TALK-1/-2 and THIK-1/-2). Notably, the NCA binding site overlaps with the promiscuous inhibitor site in hERG and, thus, targeting this NCA site might represent a promising approach to circumvent the drug-induced long QT syndrome currently a serious burden in drug development (12). However, the identified poly-pharmacology also represents a challenge for the development of any NCA based compound into a highly subtype-specific K^+ channel agonist. Nevertheless, structural differences between K_{2P}, hERG and BK_{Ca} channel may still permit a rational drug design that reduces this promiscuity. However, in some acute situations such as ischemic stroke or status epilepticus, exploiting the poly-pharmacology of NCAs to promote simultaneous opening of multiple neuroprotective K^+ channels (e.g. BK_{Ca}, TREK-1/-2, TRAAK, and THIK-1/-2), may even be beneficial.

Supplementary Material

Refer to Web version on PubMed Central for supplementary material.

Acknowledgments

We thank Florian Lesage for the THIK-1 and THIK-2 K_{2P} channel clones. We also thank Mark A. Hollywood for providing the BK_{Ca} activator GoSlo-SR-5-6. Further we thank Jana Kusch for initially testing the BL-1249 effect on CNGA1 channels. We thank all members of our respective laboratories for technical support and comments on the manuscript.

Funding: T.B. and B.L.d.G. were supported by the DFG, B.F. was supported by the DFG (SFB746, TRR 152, EXC 294, 2189), S.J.T. and E.P.C were supported by a BBSRC Industrial Partnership Award (BB/N009274/1) and LJC by a Wellcome Trust (OXION) PhD studentship. A.M. was funded by the EPSRC Life Sciences Interface Doctoral Training Centre, A.C.W.P. and E.P.C. are members of the SGC (Charity ref: 1097737) funded by AbbVie, Bayer Pharma AG, Boehringer Ingelheim, the Canada Foundation for Innovation, Genome Canada, Janssen, Merck KGaA, MSD, Novartis, the Ontario Ministry of Economic Development and Innovation, Pfizer, São Paulo Research Foundation-FAPESP and Takeda, as well as the Innovative Medicines Initiative Joint Undertaking ULTRA-DD grant 115766 and the Wellcome Trust106169/Z/14/Z. D.C.P. was an employee of Pfizer (present address: Curadev Pharma Ltd., Sandwich Kent, UK). We thank Diamond Light Source Ltd and their staff for access to the macromolecular crystallography beamlines. We also acknowledge the North-German Supercomputing Alliance (HLRN) for providing High Performance Computing (HPC) resources that have contributed to the research results reported in this paper.

References

1. Judge SIV, Smith PJ, Stewart PE, Bever CT. Potassium channel blockers and openers as CNS neurologic therapeutic agents. Recent Pat CNS Drug Discov. 2007; 2:200–28. [PubMed: 18221232]
2. Vyas VK, Parikh P, Ramani J, Ghate M. Medicinal Chemistry of Potassium Channel Modulators: An update of Recent Progress (2011-2017). Curr Med Chem. 2018; 25
3. Hou S, Heinemann SH, Hoshi T. Modulation of BKCa channel gating by endogenous signaling molecules. Physiology (Bethesda). 2009; 24:26–35. [PubMed: 19196649]

4. Niemeyer MI, Cid LP, Gonzalez W, Sepúlveda FV. Gating, Regulation, and Structure in K2P K+ Channels: In Varietate Concordia? Mol Pharmacol. 2016; 90:309–317. [PubMed: 27268784]
5. Sepúlveda FV, Pablo Cid L, Teulon J, Niemeyer MI. Molecular Aspects of Structure, Gating, and Physiology of pH-Sensitive Background K_{2P} and Kir K^+ -Transport Channels. Physiol Rev. 2015; 95:179–217. [PubMed: 25540142]
6. Yellen G. The voltage-gated potassium channels and their relatives. Nature. 2002; 419:35–42. [PubMed: 12214225]
7. Piechotta PL, et al. The pore structure and gating mechanism of K2P channels. EMBO J. 2011; 30:3607–19. [PubMed: 21822218]
8. Bagriantsev SN, Peyronnet R, Clark KA, Honoré E, Minor DL. Multiple modalities converge on a common gate to control K2P channel function. EMBO J. 2011; 30:3594–606. [PubMed: 21765396]
9. Wilkens CM, Aldrich RW. State-independent block of BK channels by an intracellular quaternary ammonium. J Gen Physiol. 2006; 128:347–364. [PubMed: 16940557]
10. Zhou Y, Xia X-M, Lingle CJ. Cysteine scanning and modification reveal major differences between BK channels and Kv channels in the inner pore region. Proc Natl Acad Sci U S A. 2011; 108:12161–12166. [PubMed: 21730134]
11. Smith PL, Baukrowitz T, Yellen G. The inward rectification mechanism of the HERG cardiac potassium channel. Nature. 1996; 379:833–836. [PubMed: 8587608]
12. Vandenberg JI, Perozo E, Allen TW. Towards a Structural View of Drug Binding to hERG K+ Channels. Trends Pharmacol Sci. 2017; 38:899–907. [PubMed: 28711156]
13. Pope L, et al. ACS Chem Neurosci.
14. Zhou J, et al. Novel potent human ether-a-go-go-related gene (hERG) potassium channel enhancers and their in vitro antiarrhythmic activity. Mol Pharmacol. 2005; 68:876–884. [PubMed: 15976038]
15. Bentzen BH, et al. The small molecule NS11021 is a potent and specific activator of Ca2+-activated big-conductance K+ channels. Mol Pharmacol. 2007; 72:1033–1044. [PubMed: 17636045]
16. Lenaeus MJ, Burdette D, Wagner T, Focia PJ, Gross A. Structures of KcsA in complex with symmetrical quaternary ammonium compounds reveal a hydrophobic binding site. Biochemistry. 2014; 53:5365–5373. [PubMed: 25093676]
17. Schewe M, et al. A Non-canonical Voltage-Sensing Mechanism Controls Gating in K2P K(+) Channels. Cell. 2016; 164:937–49. [PubMed: 26919430]
18. McCoy JG, Nimigean CM. Structural correlates of selectivity and inactivation in potassium channels. Biochim Biophys Acta. 2012; 1818:272–285. [PubMed: 21958666]
19. Dong YY, et al. K2P channel gating mechanisms revealed by structures of TREK-2 and a complex with Prozac. Science. 2015; 347:1256–1259. [PubMed: 25766236]
20. Rapedius M, et al. State-independent intracellular access of quaternary ammonium blockers to the pore of TREK-1. Channels. 2012; 6:473–478. [PubMed: 22991046]
21. Zhuo R-G. et al. Intersubunit Concerted Cooperative and cis-Type Mechanisms Modulate Allosteric Gating in Two-Pore-Domain Potassium Channel TREK-2. Front Cell Neurosci. 2016; 10:127. [PubMed: 27242438]
22. Lolicato M, et al. K2P2.1 (TREK-1)–activator complexes reveal a cryptic selectivity filter binding site. Nature. 2017; 547:364–368. [PubMed: 28693035]
23. Kopec W, et al. Direct knock-on of desolvated ions governs strict ion selectivity in K+ channels. Nat Chem. 2018; 10:813–820. [PubMed: 30030538]
24. Clausen MV, Jarerattanachat V, Carpenter EP, Sansom MSP, Tucker SJ. Asymmetric mechanosensitivity in a eukaryotic ion channel. Proc Natl Acad Sci U S A. 2017; 114:E8343–E8351. [PubMed: 28923939]
25. Kang D, Choe C, Kim D. Thermosensitivity of the two-pore domain K+ channels TREK-2 and TRAAK. J Physiol. 2005; 564:103–116. [PubMed: 15677687]
26. Zhou M, MacKinnon R. A mutant KcsA K(+) channel with altered conduction properties and selectivity filter ion distribution. J Mol Biol. 2004; 338:839–846. [PubMed: 15099749]

27. Bagriantsev SN, et al. A high-throughput functional screen identifies small molecule regulators of temperature- and mechano-sensitive K2P channels. ACS Chem Biol. 2013; 8:1841–51. [PubMed: 23738709]

28. Minieri L, et al. The inhibitor of volume-regulated anion channels DCPIB activates TREK potassium channels in cultured astrocytes. Br J Pharmacol. 2013; 168:1240–1254. [PubMed: 23072356]

29. Gordon E, et al. 2-[2-(3,4-dichloro-phenyl)-2,3-dihydro-1H-isoindol-5-ylamino]-nicotinic acid (PD-307243) causes instantaneous current through human ether-a-go-go-related gene potassium channels. Mol Pharmacol. 2008; 73:639–651. [PubMed: 18042732]

30. Hansen RS, et al. Biophysical characterization of the new human ether-a-go-go-related gene channel opener NS3623 [N-(4-bromo-2-(1H-tetrazol-5-yl)-phenyl)-N'-(3'-trifluoromethylphenyl)urea]. Mol Pharmacol. 2006; 70:1319–1329. [PubMed: 16825484]

31. Roy S, et al. Structure-activity relationships of a novel group of large-conductance Ca(2+)-activated K(+) (BK) channel modulators: the GoSlo-SR family. ChemMedChem. 2012; 7:1763–9. [PubMed: 22930560]

32. Wang W, MacKinnon R. Cryo-EM Structure of the Open Human Ether-a-go-go-Related K(+) Channel hERG. Cell. 2017; 169:422–430.e10. [PubMed: 28431243]

33. Pau V, Zhou Y, Ramu Y, Xu Y, Lu Z. Crystal structure of an inactivated mutant mammalian voltage-gated K(+) channel. Nat Struct Mol Biol. 2017; 24:857–865. [PubMed: 28846092]

34. Yang H, Zhang G, Cui J. BK channels: multiple sensors, one activation gate. Front Physiol. 2015; 6:29. [PubMed: 25705194]

Europe PMC Funders Author Manuscripts

One sentence summary

A class of negatively charged compounds activate structurally distinct K^+ channels via a conserved mechanism.

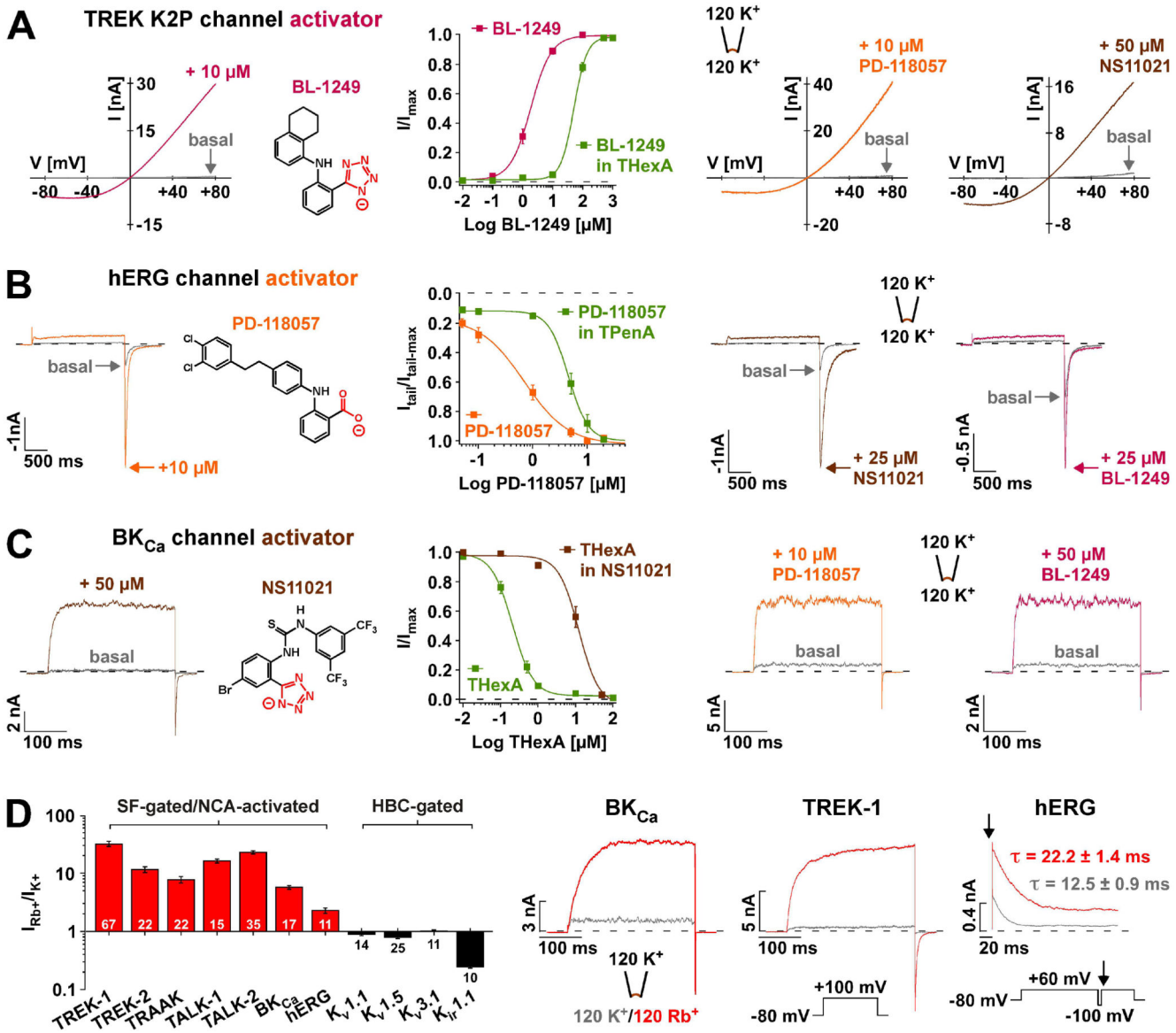

Fig. 1. Negatively charged activators (NCAs) open SF-gated K^+ channels via a similar site.

(**A**) Representative TREK-1 channel currents recorded in inside-out (i-o) patches evoked by voltage ramps in the absence (basal) and presence of the indicated compounds. BL-1249 (compound structure depicted) dose-response curves represent currents at +40 mV ± 5 µM THexA that produced 77 ± 6 % inhibition of basal currents (n ≥ 8). (**B**) hERG channel currents (voltage steps from -80 mV to +60 mV) in i-o patches ± the indicated compounds; arrows indicate peak tail current amplitudes at -100 mV. PD-118057 dose-response curves represent normalized tail currents ± 1 µM TPenA that produced 91 ± 1 % inhibition of basal currents (n ≥ 6). (**C**) BK_{Ca} channel currents (voltage steps from a holding potential of -80 mV to +100 mV (zero Ca^{2+})) in i-o patches ± the indicated compounds. THexA inhibition represents currents at +100 mV ± 50 µM NS11021 (compound structure depicted; n ≥ 11). (**D**) Bars ± S.E.M represent fold change of outward currents upon exchange of intracellular

Europe PMC Funders Author Manuscripts

K^+ by Rb^+ for K_{2P} and BK_{Ca} channels (+100 mV), for hERG, $K_v1.1$, $K_v1.5$, $K_v3.1$ channels (+60 mV) and $K_{ir}1.1$ channels (+40 mV). The channels are grouped as either SF-gated/NCA-activated or HBC (helix-bundle crossing)-gated. (**E**) Representative traces of Rb^+ activation for BK_{Ca}, TREK-1 and hERG channels using indicated protocols (arrow indicates the starting point of hERG inactivation after inactivation recovery (at -100 mV)). **τ** values from mono-exponential fits to inactivation time course ($n \geq 12$).

Europe PMC Funders Author Manuscripts

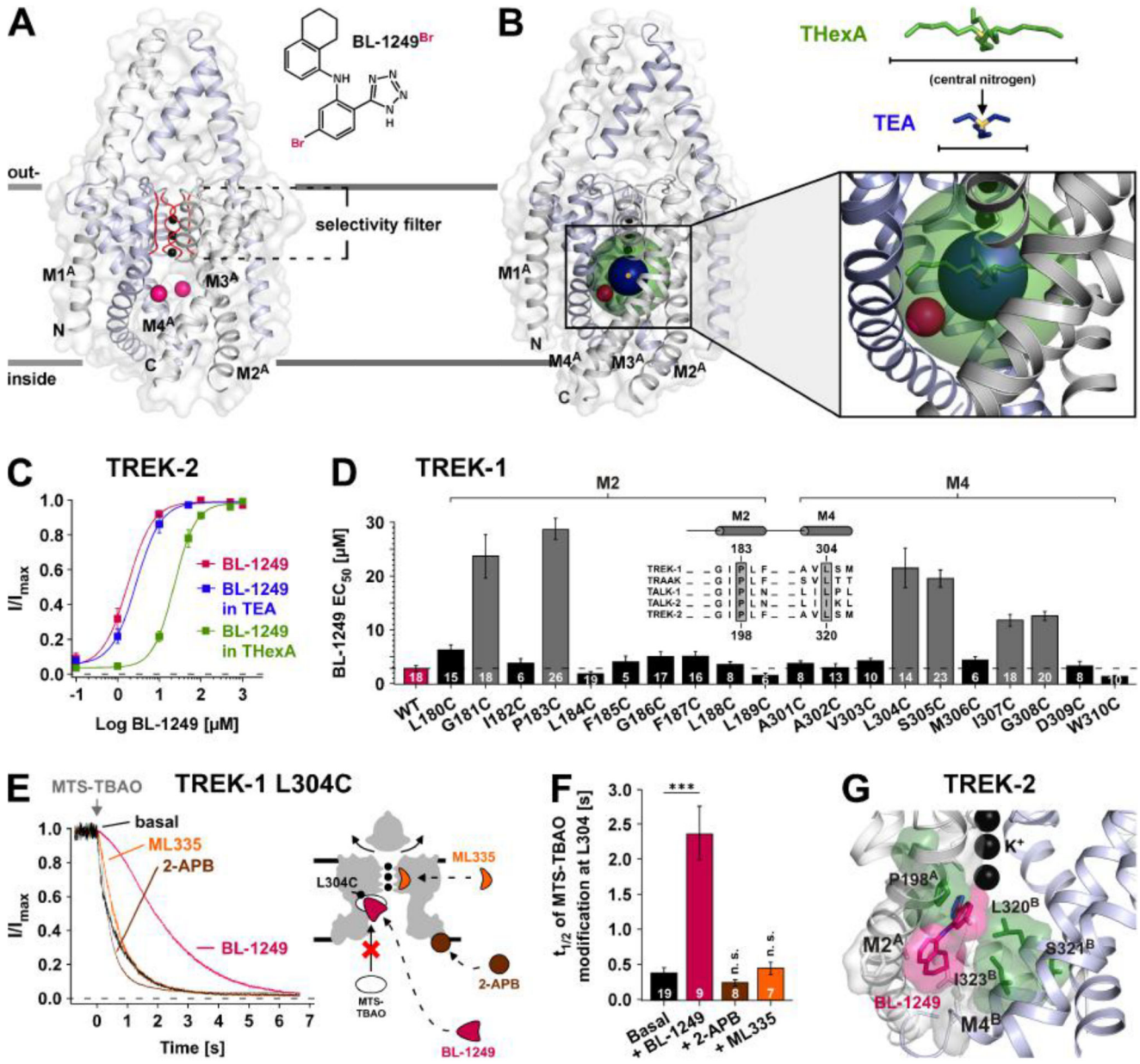

Fig. 2. Identification of the BL-1249 binding site in TREK K_{2P} channels.

(**A**) The structure depicts TREK-2 (PDB ID: 4XDJ), with pink spheres representing the positions of Br atoms in a brominated BL-1249 derivate (BL-1249^{Br}) obtained by co-crystallization of TREK-2 and BL-1249^{Br} (see also fig. S3). With this medium resolution data only the Br atoms were identified, as they gave peaks in anomalous difference maps. (**B**) The same structure also showing spherical representations of THexA (green) and TEA (dark blue) with their central nitrogen atoms (yellow). Their positions are based on the crystal structures of KcsA with QA^{+}s (16). Note the Br atoms (pink) are within the sphere of THexA, but not of TEA. (**C**) BL-1249 dose-response curves for TREK-2 ± 100 mM TEA (n ≥ 12) or 5 μM THexA (n ≥ 13) (TEA and THexA produce 74 ± 3 % and 83 ± 2 % basal current inhibition, respectively). (**D**) Scanning mutagenesis of M2 and M4 helices showing

Europe PMC Funders Author Manuscripts

BL-1249 EC_{50} values ± S.E.M determined at +40 mV; inset shows a K_{2P} channel alignment for channels strongly activated by BL-1249 (see also fig. S1D) with residues homologous to TREK-1 P183 and L304 highlighted. (**E**) Time courses of 10 μM MTS-TBAO cysteine modification of L304C in TREK-1 before and after maximal activation by BL-1249 (50 μM), ML335 (50 μM) and 2-APB (1 mM) (left panel). Cartoon depicts TREK-1 with predicted drug binding sites relative to position of residue L304C. (**F**) Time values ± S.E.M for half maximal MTS-TBAO modification inhibition ($t_{1/2}$) in presence of different agonists. (**G**) Representation of favoured binding pose of BL-1249 (pink) in TREK-2 along with location of the TREK-1 corresponding mutations (green) that reduce BL-1249 activation.

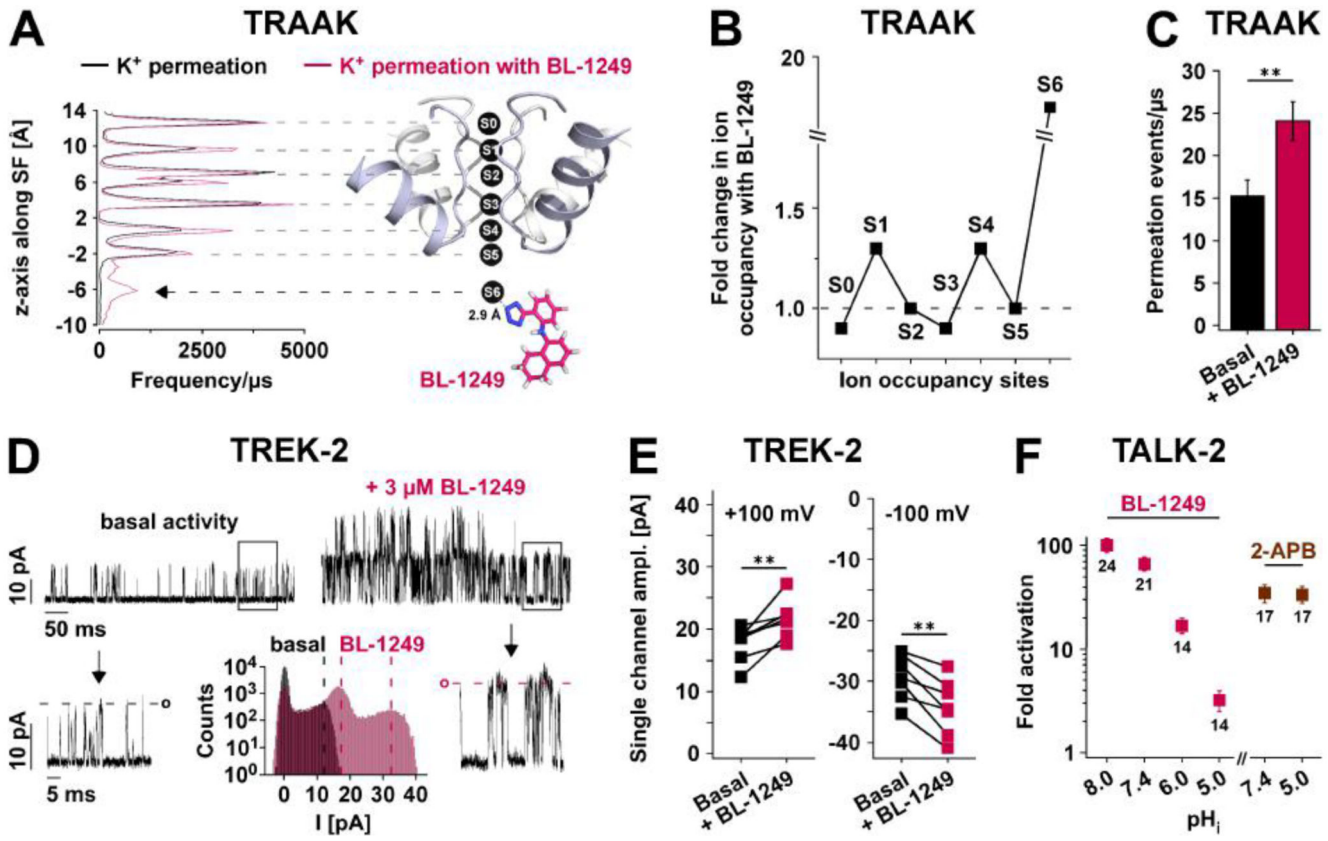

Fig. 3. Effects of BL-1249 on pore K^+ occupancy and permeation.

(**A**) Ion occupancy (frequence/µs) of K^+ binding sites (S0 - S6) obtained from permeation MD simulations of TRAAK ± BL-1249, with BL-1249 adopting the identical position in TREK-2 (Fig. 2G), i.e. the negatively charged tetrazole ring (blue) in close proximity to the S6 K^+ ion. Coordinates were saved every 40 ps. Black arrow points to the increase in S6 K^+ occupancy. (**B**) Fold change in ion occupancy for S0 - S6 sites. (**C**) Bars represent permeation events/µs from independent 200 ns MD simulations without (n = 50) and with BL-1249 (n = 30). (**D**) Single channel TREK-2 currents recorded at +80 mV from i-o patches before (basal) and after 3 µMBL-1249 with arrows pointing to expanded scales of framed sections. Lower middle panel depicts current amplitude histograms ± 3 µM BL-1249 from i-o patches with ≤ 2 active channels (note the righthand peak represents the amplitude of two BL-1249-activated channels). Dotted lines indicate the single channel amplitude maxima ± BL-1249. (**E**) Paired single channel current amplitudes before and after 3 µM BL-1249 (n = 7). (**F**) Fold activation of TALK-2 currents in i-o patches with 50 µM BL-1249 or 1 mM 2-APB applied at the indicated pH_i values.

Europe PMC Funders Author Manuscripts

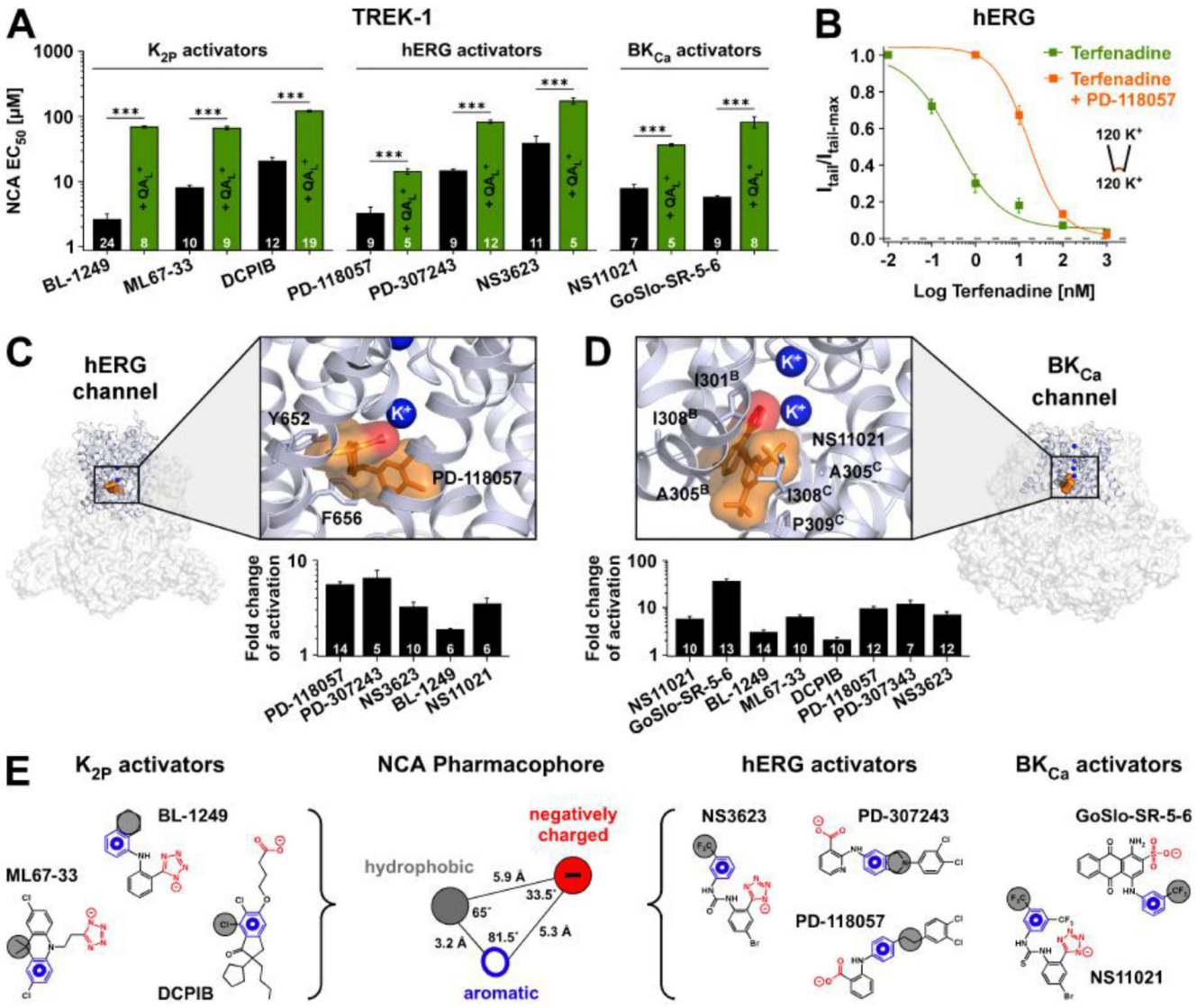

Fig. 4. NCA binding sites and common pharmacophore.

(**A**) EC_{50} values (at +40 mV) for TREK-1 activation with compounds described as activators of either K_{2P}, hERG or BK_{Ca} channels. Competitive antagonism is seen in presence of QA_L^+ (either THexA or TPenA which produce ~70 - 80 % inhibition of respective basal K^+ currents). (**B**) Terfenadine inhibition of hERG channels ± 10 μM PD-118057. (**C**) Structure of the hERG channel (PDB ID: 5VA1) with the pore region expanded. This region was used for molecular docking and MD simulations to obtain the favoured binding pose of PD-118057 (orange). Terfenadine interacting residues are highlighted. Note the carboxylate group (red) interacts with a K^+ ion below the SF (see also fig. S7D); bar chart below represents fold activation of hERG tail currents at -100 mV with 10 μM of the indicated compounds. (**D**) Similar to (**C**) but for the BK_{Ca} channel (PDB ID: 5TJI) showing the favoured binding pose of NS11021 (orange) where the tetrazole group (red) interacts with a K^+ ion below the SF and residues in proximity to NS11021 highlighted. The bar chart below shows fold activation of BK_{Ca} at +100 mV with 10 μM of the indicated compounds (at zero

Europe PMC Funders Author Manuscripts

Ca^{2+}). (**E**) Representation of the K_{2P}, hERG and BK_{Ca} activators used to generate a common NCA pharmacophore consisting of aromatic (blue), hydrophobic (gray) and acidic (red) moieties with distances and angles as depicted.

Europe PMC Funders Author Manuscripts